Performance of a Microstrip-coupled TES Imaging Module for CMB Polarimetry

Michael D. Audley[1,*], Dorota Glowacka[1], David J. Goldie[1], Vassilka Tsaneva[1], Stafford Withington[1], Lucio Piccirillo[2], Giampaolo Pisano[2], Paul Grimes[3], Ghassan Yassin[3], Peter A. R. Ade[4], C. North[4], Kent D. Irwin[5], and Mark Halpern[6]
[1]*Cavendish Laboratory, University of Cambridge, United Kingdom*
[2]*University of Manchester, United Kingdom*
[3]*University of Oxford, United Kingdom*
[4]*Cardiff University, Cardiff, United Kingdom*
[5]*National Institute of Standards and Technology, Boulder CO, United States of America*
[6]*University of British Columbia, Vancouver, Canada*
M.D. Audley is now with the Space Research Organization of the Netherlands
V. Tsaneva is now with the University of Cologne, Germany
*Contact: audley@physics.org

***Abstract*— We have developed a 16-element, 97GHz, low-noise Transition Edge Sensor (TES) module that can be packed easily into large-format polarimetric imaging arrays. The technology was developed originally for the low-frequency instrument of the CLOVER experiment, which was aimed at searching for the signature of primordial gravitational waves in the polarisation state of the Cosmic Microwave Background Radiation. Each module contains 16 slotline and microstrip-coupled TES bolometers, allowing eight polarimetric pixels with external waveguide OMTs, along with time-domain multiplexed SQUID readout. Here we describe the design of the modules, and explain how they were realised in practice, detailing some of the technology developed along the way. Performance was measured by following two parallel paths: (i) detailed characterisation of individual detectors using an exceedingly well understood, fully modelled, analogue SQUID readout system, and (ii) simultaneous measurements of the entire module using CLOVER's multichannel readout electronics. We describe the results of measurements on one of the modules, with an emphasis on uniformity of performance, and we assess the effect of non-uniformity on the operation of a complete array. Although the technology was developed in the context of CLOVER, the work has consequences for many instruments including future space telescopes such as BPol.**

I. Introduction

A. Scientific Motivation

Thomson scattering of radiation in the early Universe can lead to linear polarization [1] in the cosmic microwave background (CMB). The polarization depends on density fluctuations, and thus carries cosmological information which is complementary to the well-studied temperature anisotropies of the CMB. The linear polarization may be decomposed into a curl-free part and a divergence-free part, denoted E- and B-mode respectively. The ratio of the E- to B-mode polarisation r is proportional to the energy scale of inflation. The CLOVER experiment aimed to detect the signature of primordial gravitational waves in the B-mode polarisation of the CMB [2], [3] or to place an upper limit on r of 0.026 in an angular multipole range of $20 < \ell < 1000$ (8' to 10º).

B. Overview of CLOVER

The CLOVER experiment, which was cancelled at an advanced stage, is described in detail elsewhere [4], [5]. CLOVER consists of two telescopes (see Fig. 1), each with compact range antenna optics that have been designed to have extremely low sidelobes and cross-polarisation [6]. One telescope (the low-frequency or LF instrument) observes at 97 GHz and the other (the HF instrument) has a mixed focal plane containing detector modules sensitive in the 150- and 220-GHz bands.

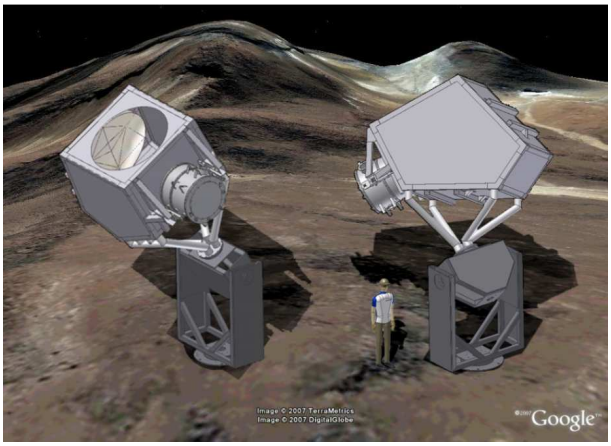

Fig. 1 Drawing of CLOVER at its site in the Atacama Desert.

To detect the extremely weak B-mode signal, CLOVER requires detectors with low enough NEP so that the instrument NEP is dominated by unavoidable sources of background photon noise ($\sim 3\times10^{-17}$ W/√Hz at 97 GHz). To achieve this sensitivity CLOVER uses bolometers with superconducting transition edge sensors (TES) [7] operating with a bath temperature of 100 mK. The detectors are cooled in two cryostats by a pulse-tube cooler, He-7 sorption fridge, and miniature dilution fridge [8]. The cryostat for the LF instrument is shown in Fig. 2.

Fig. 2 CLOVER's LF cryostat.

CLOVER's two focal planes are populated by hexagonal arrays of corrugated feedhorns (see Fig. 3).

Fig. 3 The full set of 96 corrugated feedhorns for the LF focal plane.

The low-frequency (LF) telescope's focal plane was to be populated with the detector modules discussed in this paper. The high-frequency (HF) telescope was to have a dual-frequency focal plane with a mixture of modules carrying detectors sensitive in the 150 or 220-GHz bands.

Orthomode transducers (OMT) separate the signal collected by each horn into two polarisations. In the LF telescope waveguide OMTs divide the two polarisations from each horn between two rectangular waveguides which each feed a finline-coupled detector [9]. Fig. 4 shows eight of these OMTs mounted on a LF detector module.

The high frequency channels use polarisation-sensitive detectors of a different architecture: four rectangular probes in a circular waveguide [10]. In this paper we concentrate on the LF instrument. The HF instrument was also at an advanced stage of readiness when the project was cancelled, although mass-production of the detector modules had not yet started.

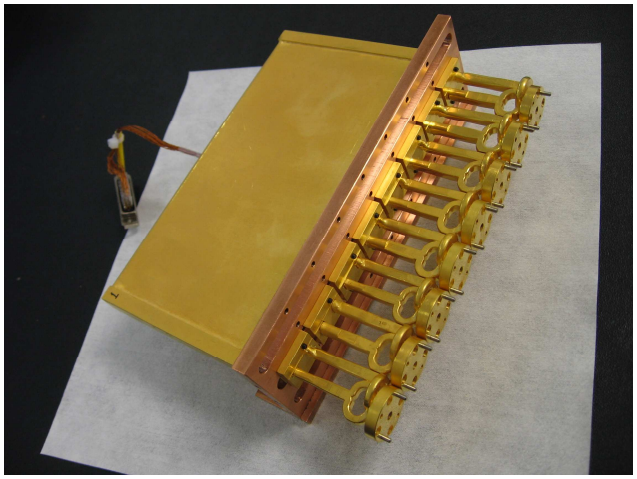

Fig. 4 LF detector module with OMTs.

Because of the large number of TESs to be read out (192 at each frequency) we use time-domain multiplexing in order to have a manageable number of wires from room temperature. The TESs are read out by 1×32 SQUID multiplexers [11], [12], [13] fabricated by the National Institute of Standards and Technology (NIST). Further amplification is provided at the cold end by SQUID series arrays [14], also fabricated by NIST.

All the multiplexer chips in each of CLOVER's two telescopes share address lines, significantly reducing the number of wires needed to room temperature. The Nyquist inductors, which provide antialiasing filtering, and the shunt resistors that provide voltage biasing, are contained in separate chips. All of these chips are mounted on a PCB at 100 mK and connections are made to the detectors by aluminium wire bonds. The SQUID series arrays are mounted in eight-chip modules which provide the necessary magnetic shielding. Because of their higher power dissipation (1 μW per series array compared with 16 nW per multiplexer chip) these modules are heat-sunk to the still of the dilution refrigerator and they are connected to the multiplexer PCB with superconducting NbTi twisted pairs. Room-temperature multi-channel electronics (MCE) developed by the University of British Columbia, provides SQUID control and readout as well as TES bias [15]. CLOVER's MCE is similar to that used by SCUBA-2 [16].

II. Detector Design

A. Requirements

For maximum sensitivity, we require that the detectors be background-limited, i.e. the contributions to the noise equivalent power (NEP) from the detectors and readout must be less than the NEP due to unavoidable sources of photon noise:

$$NEP_{det}^2 + NEP_{ro}^2 \leq NEP_{photon}^2.$$

Once the detectors are background-limited, the only way to improve the sensitivity is to increase the number of detectors. 96 pixels are needed at each frequency to meet CLOVER's sensitivity requirements. The LF instrument has two finline detectors per pixel (one for each

polarisation). In the HF instrument there is one polarisation-sensitive OMT detector chip per pixel which measures both orthogonal polarisations. Thus, the LF instrument has 192 finline detectors and the HF instrument has a total of 192 planar OMT detectors. We require a detector time constant faster than 1 ms to satisfy the scanning requirements.

Also, the detectors must be able to absorb the power incident from the sky without saturation. This power is variable and depends on the weather. The power-handling requirement is for the detectors to be able to operate for 75% of the time at the site. We have allowed a 70% margin on this to account for uncertainties in the sky background at the site. This means that our target power handling for the LF detectors is 11.4 pW, rather than the predicted background level of 6.8 pW. The detector requirements are summarised in Table I.

TABLE I

CLOVER DETECTOR REQUIREMENTS AT THE THREE OPERATING FREQUENCIES.

Centre Frequency (GHz)	97	150	220
Band (GHz)	82—112	127—172	195—255
Number of pixels	96	96	96
$NEP_{background}$ (10^{-17} W/√Hz)	2.9	4.9	8.9
Power Handling (pW)	11.4	20	32

To meet these requirements we chose targets of $T_c = 210$ mK and $G \geq 215$ pW/K for the transition temperature and thermal conductance of the LF detectors. With those values of T_c and G the phonon NEP would be ~2×10^{-17} W/√Hz. Table I shows that the sensitivity requirement is most strict on the 97-GHz detectors because of the lower sky background in the LF band. Meeting the sensitivity requirement for the 97-GHz detectors demonstrates our ability to meet the sensitivity requirement at the other two frequencies.

B. Detector Format

Rather than fabricating monolithic arrays we decided to make individual detectors so that we could guarantee a 100% functioning focal plane, which is important for meeting the sensitivity requirement. Having individual detector chips allows us to select the best ones for inclusion in the instrument. Also, because the detectors are much smaller than the horns in the focal plane, a monolithic array would have large, inactive areas between detectors, which would make fabrication of the detectors extremely inefficient. With hundreds of detectors needing to be mass-produced we decided to produce individual detectors that could be packed close together on a wafer to maximise processing efficiency.

C. TES Design

The TES films in CLOVER are Mo/Cu proximity-effect bilayers with normal copper banks to define the edges of the TES. The transitions of the bilayers can be made as sharp as 1—2 mK for high sensitivity. We can also tune the transition temperature (T_c) of the films to the desired value by choosing the film thicknesses. The transition temperature T_c and thermal conductance G of CLOVER's detectors are chosen to meet the NEP and power-handling requirements operating with a bath temperature of 100 mK.

CLOVER's bolometers are on low-stress silicon nitride islands suspended by four legs for thermal isolation (see Fig. 5). The nitride is 0.5 µm thick. The thermal conductance to the thermal bath is controlled by the four nitride legs. A microstrip carries RF power to the bolometer and is terminated by a 23-Ω AuCu resistor which dissipates the incoming power as heat that the TES can detect. A shunt resistor in parallel with the TES ensures that it is voltage biased so that it operates in the regime of strong negative electrothermal feedback. For example, if the temperature drops, so does the resistance of the TES. Since it is biased at constant voltage, this means that the current, and hence the Joule power, will increase, heating up the TES. Conversely, if the temperature increases the resistance will increase, reducing the current, and thus the Joule heating. This means that the TES operates at a bias point that is in a stable equilibrium. Thus, the TES is self-biasing, and the electrothermal feedback speeds up the response of the detector and cancels out temperature fluctuations, which has the effect of suppressing the noise.

Copper fingers extend from the normal copper banks most of the way across the TES from opposite edges (see Fig. 5). The purpose of these is to improve thermalisation of the TES film and suppress excess noise due to internal thermal fluctuations. The dark NEP we measure for these TESs is consistent with what we expect from the known Johnson and phonon noise sources [17].

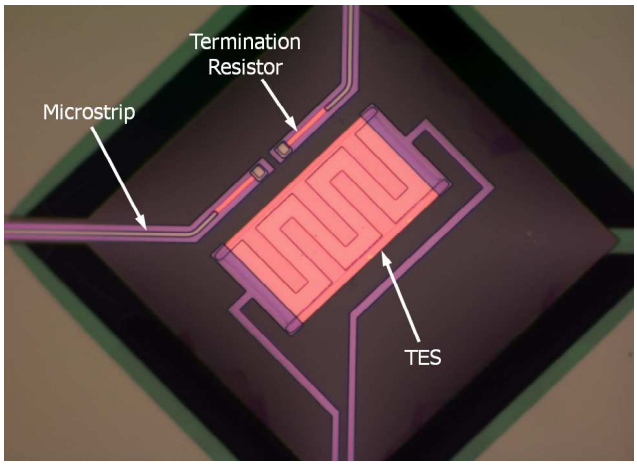

Fig. 5 CLOVER TES bolometer.

D. On-Chip Heaters

Fig. 5 shows two resistors terminating microstrips on the nitride island. One of these carries RF power from the

sky and the other is the on-chip heater which is used to inject DC power into the device.

The TES will be driven into the normal state or saturated when enough power is incident on it. This saturation power is the sum of the bias (and heater) and sky power. The sky power is variable and depends on the weather at the site. To operate efficiently CLOVER needs to be able to observe when the sky background power is high without losing the ability to observe in good weather when it is low. Also, for best performance the power incident on the detectors should be kept approximately constant so that their responsivity does not vary. The on-chip heaters are used to compensate for changes in the sky background. The heater power is increased in good weather when the sky opacity is low and decreased in bad weather when the sky background is high so that the total power incident on the detectors remains approximately constant. The on-chip heaters are also extremely useful for calibration because they allow us to inject a known amount of DC or pulsed power directly into the detectors.

E. RF Design

Fig. 6 shows one of CLOVER's 97-GHz detector chips. The chip sits in a rectangular waveguide that has small support slots cut in its walls. A unilateral finline transition [18] couples RF power from the waveguide to a slotline. A closer view of the transition is shown in Fig. 7. The slotline is coupled to a microstrip by a radial-stub transition. The microstrip is terminated on the silicon nitride island by a matched resistor where the RF power is detected by the TES. The finline has serrations where the chip sits in the support slots to prevent the propagation of higher-order modes. The measured optical efficiency of these detectors is about 60%.

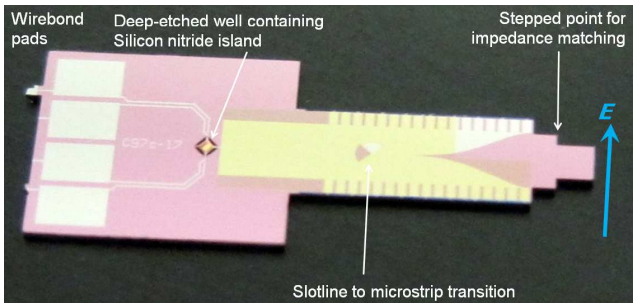

Fig. 6 CLOVER 97-GHz detector chip. The chip is 10 mm long.

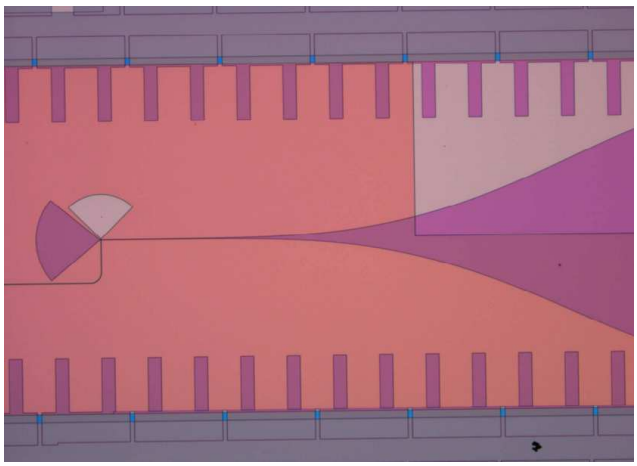

Fig. 7 The unilateral finline and the slotline to microstrip transition.

F. Detector Fabrication

The detectors are fabricated [19] on 2" silicon wafers that are 225 µm thick (see Fig. 8). The overall yield is very high and we have already mass produced all of the detectors needed to populate the LF focal plane. We have found no evidence of any change in the Mo/Cu TES properties on a timescale of years and after numerous thermal cycles.

The chip outline and the well in which the nitride island sits are defined by deep reactive ion etching (DRIE). All of the processing steps are carried out in the Detector and Optical Physics Group in the Cavendish Laboratory at Cambridge, except for the DRIE, which is done at the Scottish Microelectronics Centre in Edinburgh.

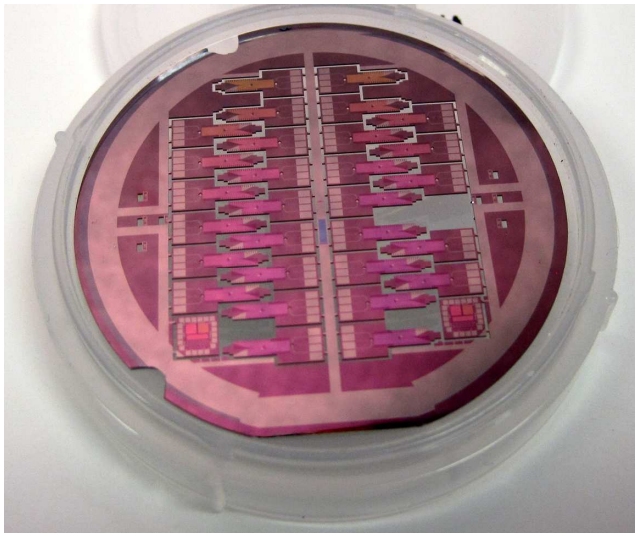

Fig. 8 30 detectors fabricated on a 2" wafer.

III. Detector Packaging

A. Detector Mounting

In order to take advantage of the fact that we are using discrete detectors that can be replaced it is necessary to mount them in such a way that they can be easily replaced in a module without disturbing the others. We thus mounted each detector chip on its own individual

chipholder as shown in Fig. 9. The chipholders are made of gold-plated copper and are fixed to the detector block with brass screws. The detector chips are glued to the chipholders using Stycast 1266 epoxy. The chipholders have been carefully designed to prevent the adhesive spreading to places where it might cause problems.

With this mounting scheme it is possible to replace individual detectors in a module without disturbing the others. This means that once we have characterised the detectors we can rearrange them, replacing some if desired, according to their properties to optimise the performance of the array.

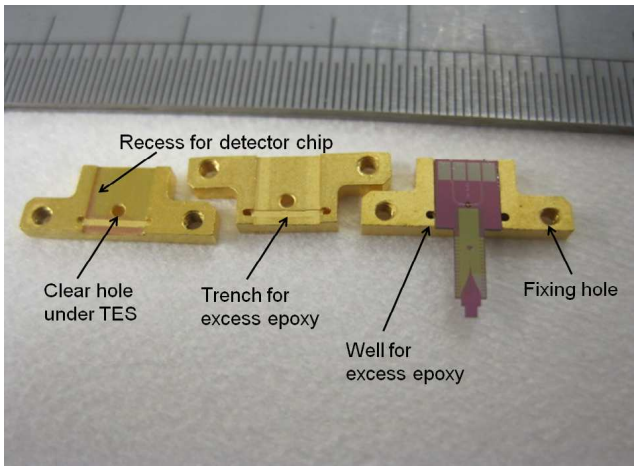

Fig. 9 Individual chipholders showing features for controlling spread of epoxy.

B. LF Module design

The finline detectors are packaged in linear modules containing 16 detectors (Fig. 10, Fig. 11). The detector block comes in two halves, upper and lower. When these are put together they form split-block waveguides (Fig. 12), into which the finlines protrude. The edges of the finlines stick into shallow slots in the sides of the waveguides for grounding. To prevent unwanted modes from propagating the WR10 waveguide is tapered to a reduced height of 1.1 mm (from 1.27 mm).

In the design of the detector module careful attention has been paid to protecting the detector chips from the effects of differential thermal contraction.

Aluminium wire bonds provide electrical connections from the detector chip to a PCB carrying the multiplexer, inductors, and shunt resistors. These three chips are held in place on the PCB with G-10 clamps. The PCB has gold-plated copper tracks and as much of the copper as possible is left on the board to help with heatsinking. The gold is deposited by electroplating in order to avoid the use of a nickel undercoat. The traces are tinned with solder to make them superconducting. The PCB is enclosed in a copper can (Fig. 13) and the module is covered with niobium foil for magnetic shielding.

This scheme has the apparent disadvantage that it under-uses the 1×32 multiplexer chips by a factor of two, increasing the number needed. However, because we are not using all of the first-stage SQUIDs on a multiplexer chip, we can connect the detectors to those SQUIDs that have the most similar critical currents. This optimises the first-stage SQUID biasing, reducing the noise contribution from this stage of the readout. Reducing the number of detectors multiplexed by each multiplexer chip also reduces the aliased readout noise, improving the NEP. Another advantage of under-using the multiplexer chips is that we can use multiplexer chips in which not all of the first-stage SQUIDs are functioning.

Fig. 14 and Fig. 15 show how the detector modules fit together to populate the focal plane. Individual modules can be removed from the focal plane or replaced either for maintenance, or to reconfigure the experiment. The modules have detachable handles to make removal easier.

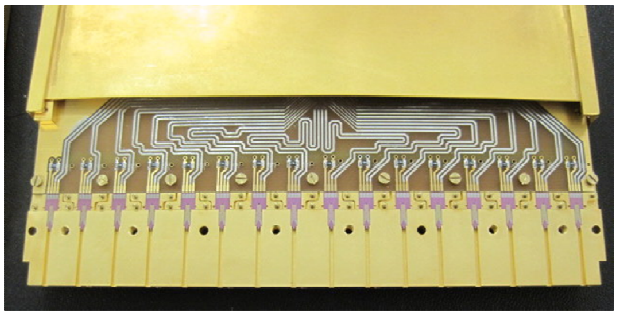

Fig. 10 LF detector module showing 16 detectors sitting in the lower block.

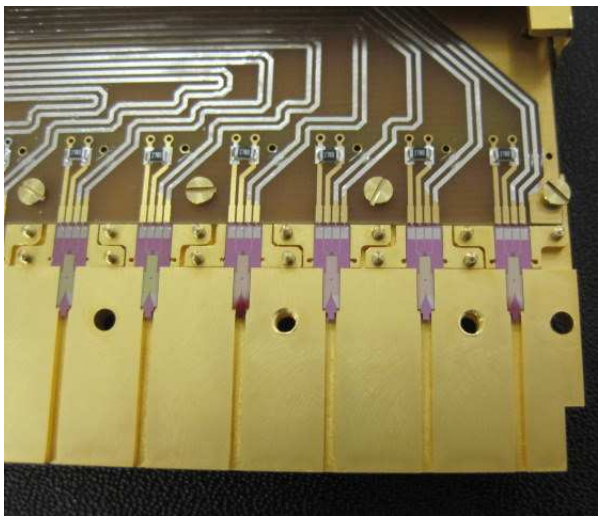

Fig. 11 Closer view of detector chips in LF module.

Fig. 12 Close-up view of assembled LF detector module showing split-block rectangular waveguides and circular alignment holes.

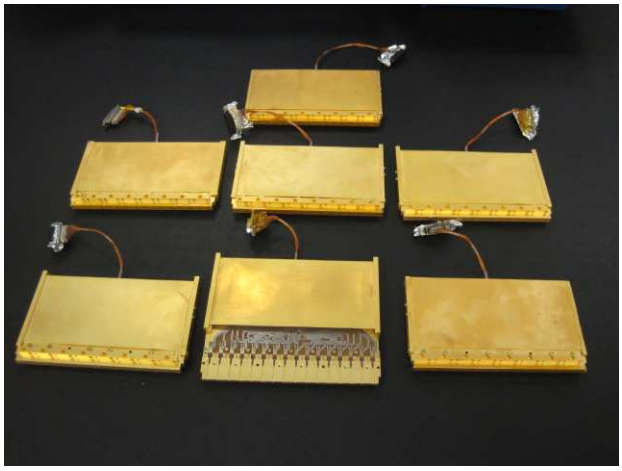

Fig. 13 Seven LF detector modules fully populated with a total of 112 detectors.

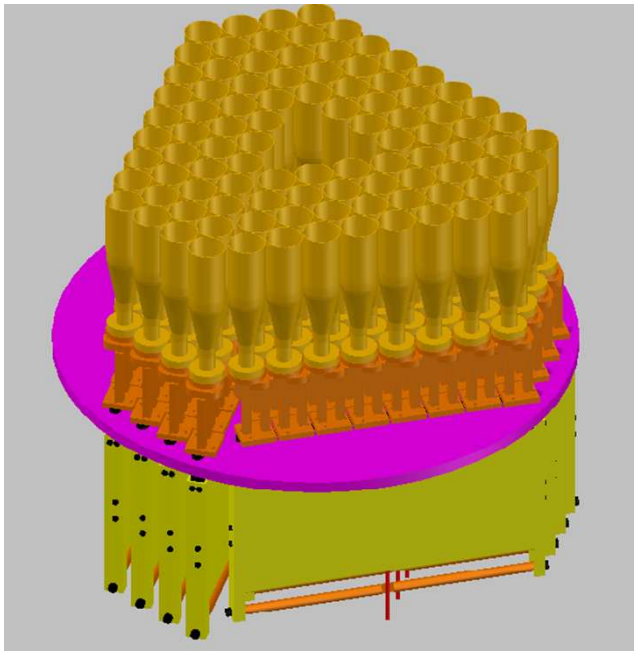

Fig. 14 Drawing of the LF focal plane populated with twelve detector modules.

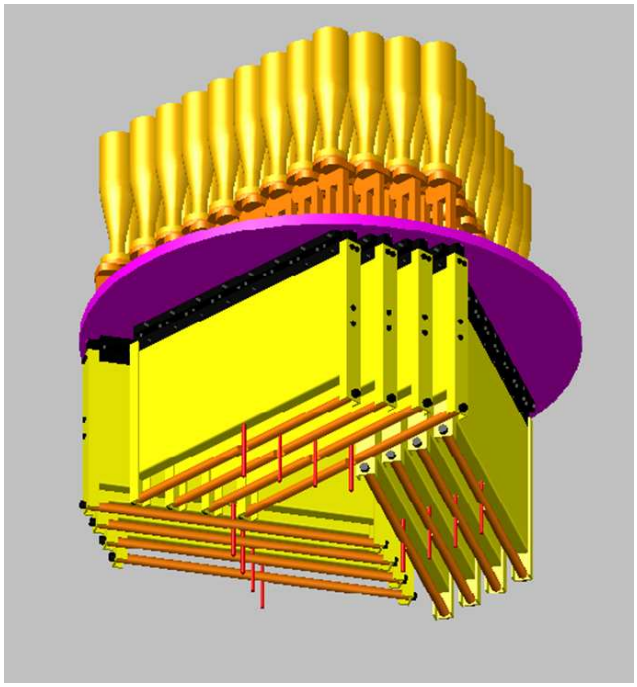

Fig. 15 Drawing of the LF focal plane viewed from the back showing how the twelve detector modules fit together.

IV. Performance

A. Testing

We have a dedicated test cryostat for mass-testing the science-grade detector modules. The cryogenics are similar to those in the final instrument, comprising a pulse-tube cooler, He-7 sorption fridge, and miniature dilution fridge. This allows us to test the detectors under realistic conditions and to validate CLOVER's cryogenics. The refrigerator can be operated remotely, and can reach a temperature of about 70 mK with a hold time of about eight hours. The cryostat has a large test volume and contains SQUID series arrays and associated wiring to read out up to eight detector modules or 128 TESs at once.

There is an internal black-body illuminator for optical tests. This illuminator has a conical radiator for high efficiency and two low-pass filters for defining the bandpass. We have paid careful attention to the thermal design of this illuminator to minimise its effect on the thermal performance of the refrigerator. The filters are mounted on nested radiation shields and these shields are heatsunk at 350 mK and 1 K stages of the He-7 sorption fridge.

The test bed also has two parallel sets of warm readout electronics (the MCE and an analogue system) so that we can characterise fully the entire readout chain from the detectors up to room temperature. Unlike the MCE, the analogue electronics does not multiplex, but can be switched between three columns and three rows. However, it is more versatile and convenient for characterising the TESs and SQUIDs. For example, it can lock on any of the three SQUID stages, while the MCE is designed to lock on the first-stage SQUID only. In this

paper we present results obtained with both sets of electronics.

B. Results

We characterised all of the detectors in a LF module using both the analogue readout electronics and the MCE. It is important not only that the detectors have transition temperatures and conductances close to the targets of $T_c = 210$ mK and $G \geq 215$ pW/K but also that these parameters are uniform across the array. The TES bias and heater supplies are common. There are three of each for the whole array. This means that the detector parameters must be uniform enough for all of the detectors to be operated simultaneously with common TES bias and heater supplies. Fig. 16 shows the measured transition temperature for the module. The row number corresponds to the detector's position in the module. The average transition temperature is 207±7 mK.

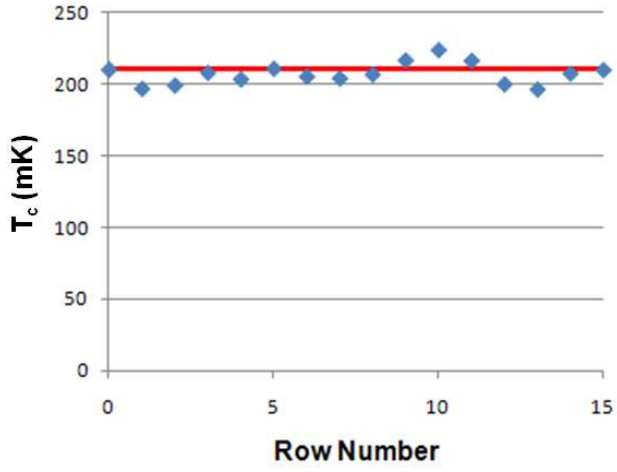

Fig. 16 Measured transition temperatures of TES detectors in module. The solid line represents the target of 210 mK

Fig. 17 shows the measured thermal conductances. The average value is G = 229±34 pW/K. The detector in position 6 has a conductance about half that of the other detectors. The reason for this is that this detector broke between the first and second thermal cycles of the module. Only two of its nitride legs were then intact so that its thermal conductance was halved. It should be noted that this is an extremely rare event: only two detectors out of hundreds have failed in this way. We have found that two thermal cycles will identify any detectors that should be replaced; no detector that survived two thermal cycles has ever failed even after numerous further cycles.

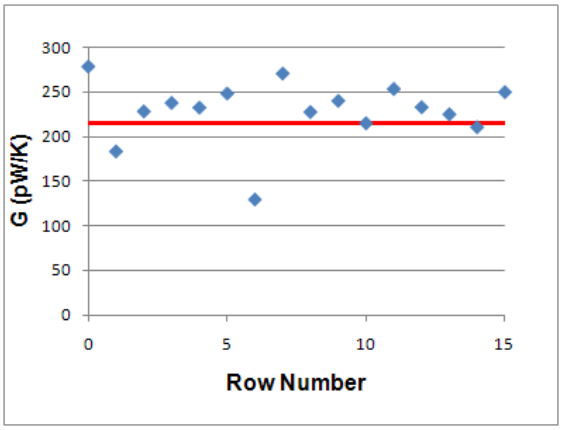

Fig. 17 Measured thermal conductances of TES detectors in module. The solid line represents the target of 215 pW/K.

Fig. 18 shows the heater power required to saturate the detectors in the module when operated with a bath temperature of 100 mK. The average value is P_{100} = 13±2 pW. When the optical efficiency of 60% is taken into account all of the detectors have power handling comfortably larger than 11.4 pW, except for the broken detector in position 6.

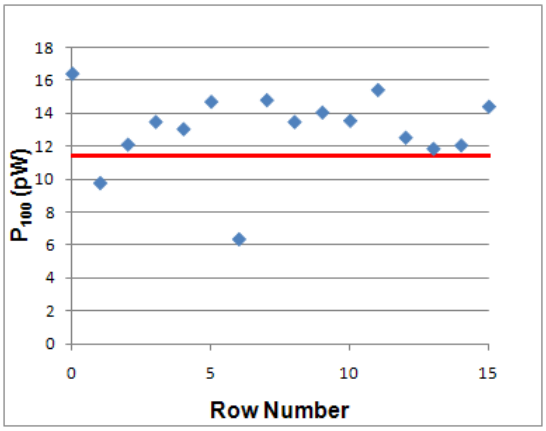

Fig. 18 Measured power handling of TES detectors in module. The solid line represents the target of 11.4 pW.

Fig. 19 shows the response of the detectors to power injected into the on-chip heaters. The heater power has been divided by the optical efficiency (60%) to show the response to incident radiation. The detectors were operated with a fixed bias of 191 nV and read out simultaneously with the MCE. The curve for each detector has a linear region where the TES is biased on its transition. The slope of this linear region is the responsivity of the detector. At higher powers the curves flatten out as each TES becomes saturated and the responsivity decreases to close to zero. The curves do not extend all the way down to zero heater power. This is because either the electrical circuit has become unstable low on the transition where the L/R time constant becomes long or the TES is in the superconducting state. The linear region of each curve shows the range of heater powers over which we can operate the detectors. The vertical solid line in Fig. 19 is the power handling target of 11.4 pW. Clearly the

detectors can be operated simultaneously over a comfortable range of heater powers around this target. We therefore conclude that the detectors are sufficiently uniform to be operated in an array.

It should be noted that we have made no attempt to select detectors with similar properties when populating this module; the 16 detectors were chosen at random before their properties were known. It has always been intended that before delivery to the telescope the detectors would be characterised and replacements made if necessary to optimise the sensitivity of the array. The fact that we obtain the required uniformity without any detector selection means that a 100% functional focal plane is readily achievable for CLOVER.

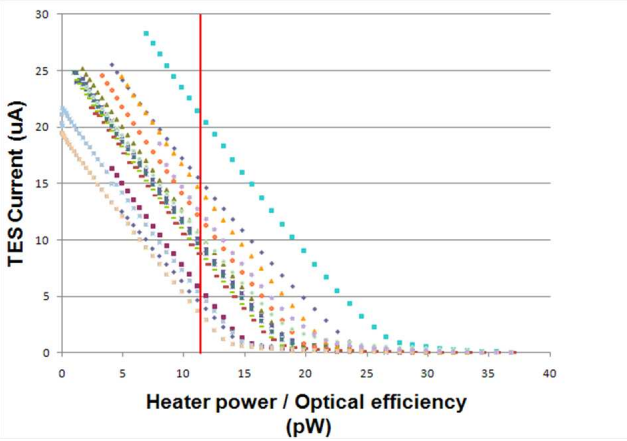

Fig. 19 Response of TES current to power injected into the on-chip heaters. The vertical line shows the 11.4-pW power-handling target.

V. Conclusions

We have successfully mass-produced all of the detectors for the LF focal plane and integrated them into detector modules. We have demonstrated that these detectors have the required power-handling, NEP, and optical efficiency for ground-based CMB polarimetry, with sufficient uniformity in the detector parameters that they can be operated simultaneously with common TES bias and heater lines.

While this paper has concentrated on the LF detector modules, it should be noted that the CLOVER team has produced an essentially complete instrument which would be expected to be very successful if deployed. Everything from detector modules, OMTs, feedhorns, filters, and readout electronics through to the mirrors and telescope mounts has been manufactured and tested and is ready for integration. Also, a large body of software has been produced for the automatic acquisition and analysis of data as well as extensive modelling work. All of this work will be relevant to any future CMB polarisation experiments.

Acknowledgment

This work was carried out for the CLOVER project, funded by the Science and Technology Research Council. The authors would like to thank Michael Crane for his contribution to device fabrication and process development, Dennis Molloy for mechanical engineering, and David Sawford for electronic and software engineering. Finally, we would like to thank all of the members of the CLOVER team for their contributions to producing a world-class instrument.

References

[1] M.J. Rees, "Polarization and Spectrum of the Primeval Radiation in an Anisotropic Universe," *Astrophysical Journal*, vol. 153, pp. L1, 1968.

[2] U. Seljak and M. Zaldarriaga, "Signature of Gravity Waves in the Polarization of the Microwave Background," *Physical Review Letters* , vol. 78, pp. 2054–2057, 1997.

[3] M. Kamionkowski, A. Kosowsky, and A. Stebbins, "A Probe of Primordial Gravity Waves and Vorticity," *Physical Review Letters*, vol. 78, pp. 2058–2061, 1997.

[4] L. Piccirillo, P. Ade, M.D. Audley, C. Baines, R. Battye, M. Brown, P. Calisse, A. Challinor, P. Ferreira, W. Gear, D.M. Glowacka, D. Goldie, P.K. Grimes, V. Haynes, B. Johnson, M. Jones, A. Lasenby, P. Leahy, S. Lewis, B. Maffei, L. Martinis, P.D. Mauskopf, S.J. Melhuish, C.E. North, D. O'Dea, G. Pisano, G. Savini, R.V. Sudiwala, A. Taylor, G. Teleberg, D. Titterington, V.N. Tsaneva, C. Tucker, and R. Watson, "The CLOVER experiment," *Proceedings of the SPIE*, vol. 7020, pp. 70201E-70201E-10, 2008.

[5] P.K. Grimes, P.A.R. Ade, M.D. Audley, C. Baines, R.A. Battye, M.L. Brown, P. Cabella, P.G. Calisse, A.D. Challinor, P.J. Diamond, W.D. Duncan, P. Ferreira, W.K. Gear, D. Glowacka, D.J. Goldie, W.F. Grainger, M. Halpern, P. Hargrave, V. Haynes, G.C. Hilton, K.D. Irwin, B.R. Johnson, M.E. Jones, A.N. Lasenby, P.J. Leahy, J. Leech, S. Lewis, B. Maffei, L. Martinis, P. Mauskopf, S.J. Melhuish, C.E. North, D. O'Dea, S.M. Parsley, L. Piccirillo, G. Pisano, C.D. Reintsema, G. Savini, R. Sudiwala, D. Sutton, A.C. Taylor, G. Teleberg, D. Titterington, V. Tsaneva, C. Tucker, R. Watson, S. Withington, G. Yassin, J. Zhang, and J. Zuntz, "Clover - Measuring the Cosmic Microwave Background B-mode Polarization", *Proceedings of the 20th International Symposium on Space Terahertz Technology*, pp. 97-106, 2009.

[6] G. Yassin, S.B. Sørenson, and P.K. Grimes, "Compact Optical Assemblies for Large-Format Imaging Arrays", *Proceedings of the 16th International Symposium on Space Terahertz Technology*, pp. 89-92, 2005.

[7] K.D. Irwin, "Phonon-Mediated Particle Detection Using Superconducting Tungsten Transition-Edge Sensors", PhD thesis, Stanford University, Stanford, California, 1995.

[8] G. Teleberg, S.T. Chase, and L. Piccirillo, "A miniature dilution refrigerator for sub-Kelvin detector arrays," *Proceedings of the SPIE*, vol. 6275, pp. 62750D, 2006.

[9] G. Pisano, L. Pietranera, K. Isaak, L. Piccirillo, B. Johnson, B. Maffei, and S. Melhuish, "A Broadband WR10 Turnstile Junction Orthomode Transducer," *IEEE Microwave Compon. Lett.,* vol. 17, pp. 286-288, 2007.

[10] P. Mauskopf, J. Zhang, P. Ade, S. Withington, and P. Grimes, "Clover Polarimetric Detector - A Novel Design of an Ortho-mode Transducer at 150 and 225 GHz", *Proceedings of Progress In Electromagnetics Research Symposium*, pp. 173-176, 2008.

[11] J.A. Chervenak, K.D. Irwin, E.N. Grossman, J. Martinis, C.D. Reintsema, and M.E. Huber, "Superconducting multiplexer for arrays of transition edge sensors, *Applied Physics Letters,* vol. 74, pp. 4043–4045, 1999.

[12] P.A.J. de Korte, J. Beyer, S. Deiker, G.C. Hilton, K.D. Irwin, M. Macintosh, S.W. Nam, C.D. Reintsema, L.R. Vale, and M.E. Huber, "Time-division superconducting quantum interference device multiplexer for transition-edge sensors," *Review of Scientific Instruments,* vol. 74, pp. 3807–3815, Aug. 2003.

[13] C.D. Reintsema, J. Beyer, S.W. Nam, S. Deiker, G.C. Hilton, K. Irwin, J. Martinis, J., Ullom, L.R. Vale, and M. Macintosh, "Prototype system for superconducting quantum interference device multiplexing of large-format transition-edge sensor arrays," *Review of Scientific Instruments,* vol. 74, pp. 4500–4508, Oct. 2003.

[14] R.P. Welty and J.M. Martinis, "Two-stage integrated SQUID amplifier with series array output," *IEEE Transactions on Applied Superconductivity,* vol. 3, pp. 2605–2608, 1993.

[15] E.S. Battistelli, M. Amiri, B. Burger, M. Halpern, S. Knotek, M. Ellis, X. Gao, D. Kelly, M. Macintosh, K. Irwin, and C. Reintsema, "Functional Description of Read-out Electronics for Time-Domain Multiplexed Bolometers for Millimeter and Sub-millimeter Astronomy," *Journal of Low Temperature Physics,* vol. 151, pp. 908–914, 2008.

[16] M.D. Audley, W.S. Holland, T. Hodson, M. MacIntosh, I. Robson, K.D. Irwin, G. Hilton, W.D. Duncan, C. Reintsema, A.J. Walton, W. Parkes, P.A.R. Ade, I. Walker, M. Fich, J. Kycia, M. Halpern, D.A. Naylor, G. Mitchell, and P. Bastien, "An update on the SCUBA-2 project," *Proceedings of the SPIE*, vol. 5498, pp. 63–77, 2004.

[17] D.J. Goldie, M.D. Audley, D.M. Glowacka, V.N. Tsaneva, and S. Withington, "Modeling and reduction of excess noise in transition edge sensor detectors," *Proceedings of the SPIE*, vol. 7020, pp. 70200K-70200K-12, 2008.

[18] G. Yassin, P.K. Grimes, O.G. King, and C.E. North, "Waveguide-to-planar circuit transition for millimetre-wave detectors," *Electronics Letters*, vol. 44, pp. 866-867, 2008.

[19] D.M. Glowacka, D.J. Goldie, S. Withington, M. Crane, V. Tsaneva, M.D. Audley, and A. Bunting, "A Fabrication Process for Microstrip-Coupled Superconducting Transition Edge Sensors Giving Highly Reproducible Device Characteristics," *Journal of Low Temperature* Physics, vol. 151, pp. 249–254, 2008.